SIMULATION OF MICROWAVE HEATING APPLIED TO THE TREATMENT OF MALIGNANT TUMORS

Marcos Enê Chaves Oliveira – menevo@deq.ufmg.br
Adriana Silva França - franca@deq.ufmg.br
DEQ/UFMG – Rua Espírito Santo 35 – 30160030 - Belo Horizonte, MG, Brazil

Abstract. *It has been known for the past century that, if malignant cells are exposed to temperatures in the range of 42 to 45^{o}C, the growth of a malignant tumor can be reduced. Therefore, the use of induced hyperthermia has been considered as a treatment for cancer patients. There are two basic forms in which hyperthermia can be employed. The conventional route is by contact with a heated medium, usually a water bath. An alternative route is to apply electromagnetic radiation such as microwaves, in which energy penetrates the body and generates heat internally. This type of treatment can be predicted and evaluated with the aid of numerical simulation. The electric component field of the microwave patterns, which is responsible for heating, can be evaluated by solving Maxwell's equations for electromagnetic wave propagation. In this paper, the electric field distribution obtained from solving these equations was coupled to the energy equation to predict the temperature distribution during microwave heating. A discussion on the applicability of Lambert's law approximation is presented. Simulation results show that the treatment is significantly affected by irradiation direction and intensity, and also by sample size, shape and rotation. The effects of blood perfusion rate were also evaluated.*

Keywords: *Finite element method, Maxwell's equations, Hyperthermia.*

1. INTRODUCTION

The treatment of malignant tumors by hyperthermia consists on submitting the pacient to temperatures in the range in the range of 42ºC to 45ºC either globally (the entire body of the pacient is exposed to high temperatures) or locally (only the affected region is exposed). Global treatment has the disadvantadges of the discomfort endured by the pacient coupled with the submission of normal cells to rigorous temperature conditions. Thus, local treatment provides a better alternative. Some of the techniques applied to hyperthermia treatments include radio frequency radiation, ultrasound, optical excitation and microwaves. The use of microwaves presents high potential, since this technique allows a more direct and localized application of heat, thus resulting in higher temperatures only in the region of the tumor and decreasing temperature effects in the normal tissue surrounding the tumor (O'Brien and Mekkaouni, 1993).

The objective of the present study was to simulate a local hyperthermia treatment using microwave heating. The finite element method was used to solve the governing equations. The electric field distribution, obtained from solving Maxwell's equations, was coupled to the energy equation to predict the temperature distribution during microwave heating. The effects of microwave power intensity, irradiation direction and form of application and sample, size, shape and orientation were evaluated.

2. METHODOLOGY

2.1 – Microwave irradiation

Evaluation of the temperature distribution in any material submitted to microwave irradiation depends on the knowledge of the electromagnetic field resulting from microwave power absorption. Several simulation studies have modeled the heat generation due to microwaves by considering that the microwave power decreases exponentialy as a function of penetration into the sample. Such approach, known as Lambert's law, can be obtained through a series of simplifications aplied to Maxwell's equations (Barringer et al., 1995). It can be evaluated according to the following expression (Datta et al., 1992).

$$Q = Q_0 e^{-d/\delta} \tag{1}$$

where Q_0 is the transmitted power flux at the surface of the material, d is the sample characteristic length and δ is the microwave penetration depth. Even though equation (1) can be easily solved, it is valid only for semi-infinite samples with dimensions much larger that the wave length. Furthermore, employment of this equation requires the estimation of Q_0, from calorimetric measurements. Another possibility is to obtain δ and Q_0 through fitting of model predictions to experimental temperature profiles δ (Ayappa et al., 1991; Barringer et al., 1995).

A more rigorous procedure to evaluate the electromagnetic field distribution consists on solving Maxwell's equations. Besides the inherent complexity of the resulting system of equations, this also requires a restriction of the simulation domain, since the electromagnetic field is distributed in both the sample and the surrounding medium. With that, appropriate boundary conditions must be applied at the restricted area (Givoli & Keller, 1989). In the present study, the simulation domain is defined as a cylindrical region involving the irradiated product, as presented in Fig. 1. Region 1 corresponds to the material being irradiated. Boundary conditions are applied on the cylinder surrounding region 2. The square region represents the location of the tumor, where higher temperatures are desired.

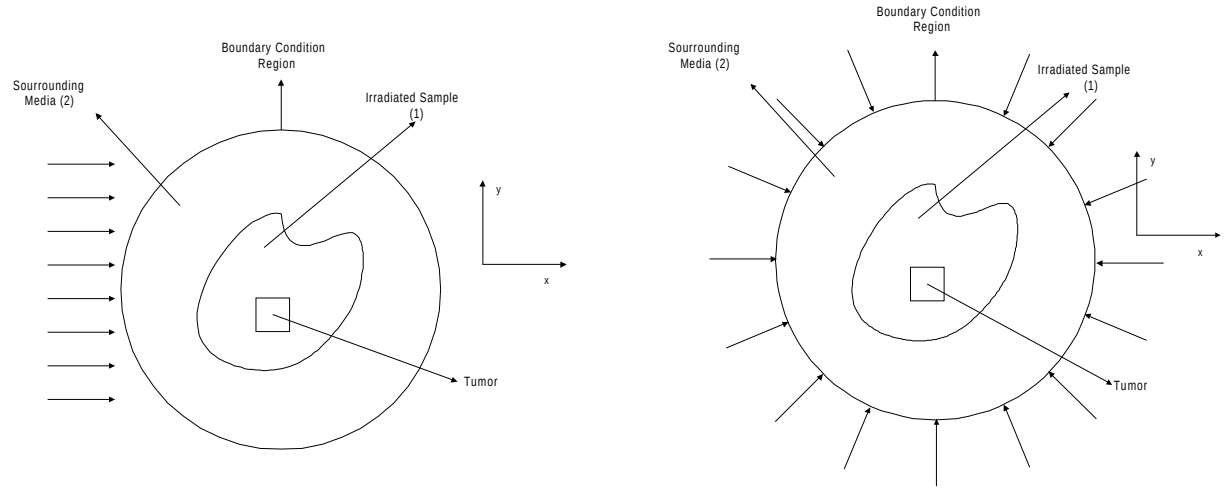

(a) (b)

Figure 1 –Simulation domain for (a) lateral and (b) radial irradiation

The electric field of the incident wave is polarized along the z-axis, and varies in both x and y directions, as shown in Fig. 2. With that, the problem can be characterized as two-dimensional.

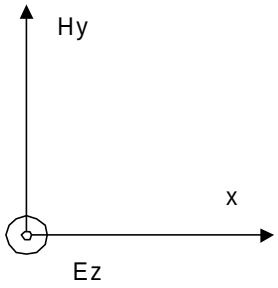

Figure 2 –TM^z polarization.

Maxwell's equations can be written as (Ramo et al., 1981).

$$\nabla \cdot B = 0 \tag{2}$$

$$\nabla \cdot D = \rho_m \tag{3}$$

$$\nabla \times \mathrm{E} = -\frac{\partial \mathrm{B}}{\partial \mathrm{t}} \tag{4}$$

$$\nabla \times \mathrm{H} = \mathrm{J} + \frac{\partial \mathrm{D}}{\partial \mathrm{t}} \tag{5}$$

with

$$J = \sigma(\omega)E(t) \tag{6}$$

$$D = \varepsilon(\omega)E(t) \tag{7}$$

$$B = \mu_m(\omega)H(t) \tag{8}$$

where B is the magnetic induction, D is the electric displacement, E is the electric field intensity, H corresponds to the magnetic field intensity, J is the current flux, ρ is the density, ω is the angular frequency, σ is the electric conductivity, ε is the permittivity, and μ is the permeability. Assuming a time dependence of the form $e^{-i\omega t}$ and applying Fourier transforms to equations (2) to (8), one can obtain the following system of equations relating the real and imaginary components of the electric field:

$$\nabla^2 E^R + E^R \psi^E - E^I \chi^E = 0 \tag{9}$$

$$\nabla^2 E^I + E^I \psi^E - E^R \chi^E = 0 \tag{10}$$

where ψ^E and χ^E are dimensionless parameters based on dielectric properties (k'and k"), k'is the dielectric constant, k'' is the relative dielectric loss, E^R is the dimensionless real electric field component and E^I corresponds to the dimensionless imaginary electric field component. Once the electric field intensity is known, the local power dissipated (Q) can be evaluated as (Ayappa et al., 1992):

$$Q = \frac{1}{2}\omega\varepsilon_0 k'' \bar{E} \cdot E^* \tag{11}$$

where E^* is the complex conjugate of $\bar{E}$, ω is the wave frequency, and ε_0 is the free space permittivity. Solution of equations (9) and (10) requires application of appropriate boundary conditions (Balanis, 1989; Givoli & Keller, 1989; Grote & Keller, 1995). The boundary conditions developed by Givoli & Keller (1989) can be applied to simulate lateral irradiation.

These conditons are exact and applied on a circular region of arbitrary size surrounding the sample. They were modified by Ayappa et al. (1992), which introduced the effect of the electromagnetic field and can be described by the following equations:

$$\frac{\partial E^R}{\partial r} = \sum \mathrm{Re}(Cn)\cos(n\phi) + \sum_n \mathrm{Re}(Dn) \int_0^{2\pi} E^R(1,\phi)\cos n(\phi-\phi')d\phi' - \sum \mathrm{Im}(Dn) \int E^I(1,\phi)\cos n(\phi-\phi')d\phi \quad (12)$$

$$\frac{\partial E^I}{\partial r} = \sum \mathrm{Im}(Cn)\cos(n\phi) + \sum_n \mathrm{Re}(Dn) \int_0^{2\pi} E^R(1,\phi)\cos n(\phi-\phi')d\phi' + \sum_n \mathrm{Im}(Dn) \int E^I(1,\phi)\cos n(\phi-\phi')d\phi \quad (13)$$

with

$$C_n = \varepsilon_n i^n k_2 \left[J_n'(k_2) - J_n(k_2) \frac{H_n^{(1)'}(k_2)}{H_n^{(1)}(k_2)} \right] \qquad \varepsilon_n = \begin{cases} 1, & n = 0 \\ 2, & \forall n > 0 \end{cases} \quad (14)$$

$$D_n = \frac{\delta_n k_2 H_n^{(1)'}(k_2)}{H_n^{(1)}(k_2)} \qquad \delta_n = \begin{cases} 1/2, & n = 0 \\ 1, & \forall n > 0 \end{cases} \quad (15)$$

where r and ϕ correspond to the radial and angular coordinates, respectively; H_n is the Hankel function of the first kind, J_n is the n-th order Bessel function of the first kind and k_2 is the wave propagation constant in region 2. The boundary conditions represented by equations (12) and (13) are not local, since the integral term depends on every point located at the boundary. In the simulations that involve radial irradiation, the boundary conditions presented by Balanis (1989) are employed.

In the present study, the direction of radiation incidence is varied in order to simulate rotation of the irradiated sample, according to the following equation:

$$\phi = \phi_0 + Va \cdot t \quad (16)$$

were ϕ represents the location of the sample at time t, ϕ_0 corresponds to the location of the sample when irradiation begins, Va is the source (or sample) angular velocity and t is the time.

2.2 –Heat transfer

Heat transfer resulting from microwave incidence over a generic solid body represented by region 1 (Fig. 1(a)) can be described by the transient heat conduction equation:

$$\rho C_p \left(\frac{\partial T}{\partial t} \right) = \frac{\partial}{\partial x}\left(k \frac{\partial T}{\partial x} \right) + \frac{\partial}{\partial y}\left(k \frac{\partial T}{\partial y} \right) + Q + W_b \quad (17)$$

where T is the temperature, C_p is the specific heat capacity, k is the thermal conductivity, W_b is the blood perfusion rate and ρ is the solid density. The heat generation term (Q) can be evaluated according to the electric field distribution resulting from solving Maxwell's equations (equation 11) or according to Lambert's law (equation 1).

2.3 –Finite element analysis

The Galerkin weighted residuals technique was employed to discretize equations (9) to (15) and (17), according to the procedure described in the standard finite element literature. A Crank-Nicolson finite differences scheme was employed for discretization of the time derivative terms.

3. RESULTS AND DISCUSSION

Simulations were performed for cylindrical tissue samples irradiated at 2800MHz with the microwaves propagating towards the right. We assumed that the values for thermophysical and dielectric tissue properties could be approximated by those obtained for meat (Table 1). The initial temperature was 27 ºC and the boundaries were isolated. Temperature isolines after 1 min heating are displayed in Fig. 3, for 0.8 and 4.0 cm radii samples.

Table 1 – Thermophysical and dielectrical properties (Ayappa et al., 1992).

Property	Frequency (MHz)	
	900	2800
k’	66.0	42.6
k’’	17.2	13.1
Density(kg / m^3)	1070	
Conductivity ($/ m.K$)	0.491	
Specific heat ($J / g.K$)	2.510	

The results presented in Fig. 3 presented good agreement with literature results (Ayappa et al., 1992), with a maximum percent difference of 3% for the larger sample. These results also show that the size of the samples significantly affects microwave heating. In smaller samples (Fig. 3 (a)), higher temperatures are concentrated in the center portion of the sample. As the sample size increases (Fig. 3 (b)), heating also becomes significant near the surface closest to microwave incidence. This type of behavior is due to the fact that in the smaller sample, the wavelenght inside the sample is approximately the same size of the sample (1.61 cm). Thus, this sample is submitted to an electromagnetic field whose intensity does not vary significantly. However, for larger samples, the ratio between wavelength and sample size diminishes and the field decay occurs near the surface, resulting in smaller values inside the sample The results presented in Fig. 3 (c) show that sample rotation leads to a more uniform temperature distribution with smaller temperature gradients throughout the material, and higher temperatures in the center of the sample.

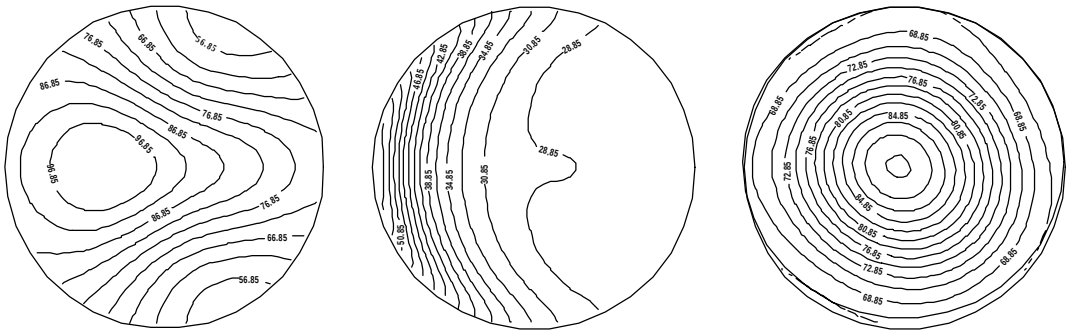

(a) (b) (c)

Figure 3 –Temperature profiles after 1 minute for static samples of (a) 0.8 and (b) 4.0 cm radii and for (c) a 0.8 cm radius sample rotating at 2 rpm

Simulations were also performed for cylindrical tissue samples of 4, 5, and 8 cm radii submitted to radial irradiation at 2800 MHz. The resulting power distributions are presented in Fig. 4 and compared to those predicted according to Lambert's law, with Q_0 estimated by solving Maxwell's equations.

The results presented in Fig. 4 show that power distributions predited by Maxwell's equations tend to agree with Lambert law predictions as the sample radius increases. The average percent difference between the two models near the sample surface (depth > 0.8 radius) was 16%, 10% and 4% for 4cm, 5cm and 8cm sample radius, respectively. It is noteworthy to point out that, even though Lambert's Law can be employed to obtain the power distribution for large samples, it is dependent of experimental parameters that are restricted to the situation being evaluated (Datta et al, 1992; Ayappa et al., 1991). Furthermore, its application is restricted to regularly shaped samples irradiated radially. Maxwell's equations are generic and its use is dependent only on the knowledge of dielectric properties, which are available for a wide range of materials. Therefore, application of Lambert's equations to simulate hyperthermia is quite restricted.

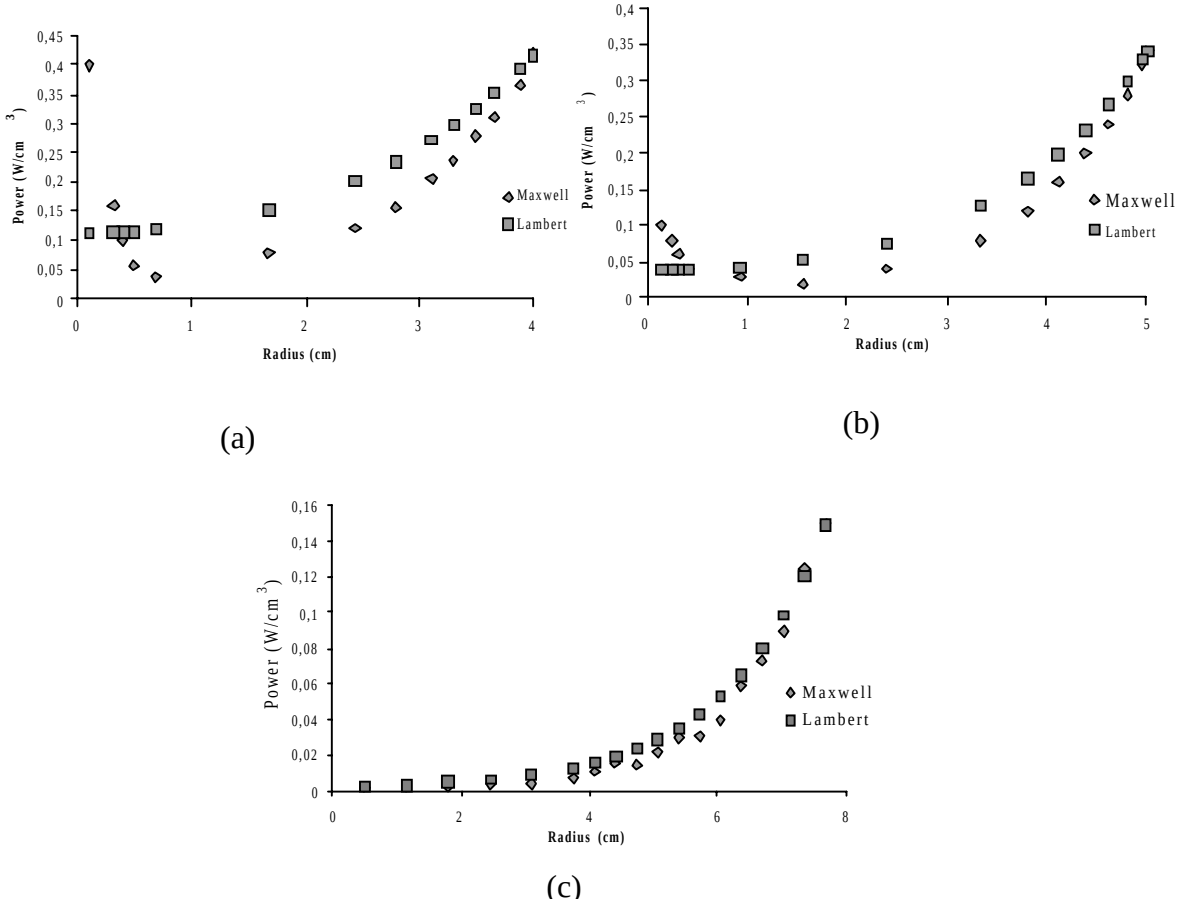

Figure 3 – Power (W/cm^3) distribution for (a) 4, (b) 5 and (c) 8 cm radii tissue samples.

Simulations were also performed for a rectangular tissue sample (5.0 x 2.5 cm) with the tumor located at the center, submitted to microwave irradiation at 0.5 W/cm^2 and 2800MHz. The initial temperature was 37 ºC, and the sample was immersed in a water bath at 37^{o}C, simulating the human body temperature. Figure 4 displays the resulting temperature distributions after 2 minutes heating.

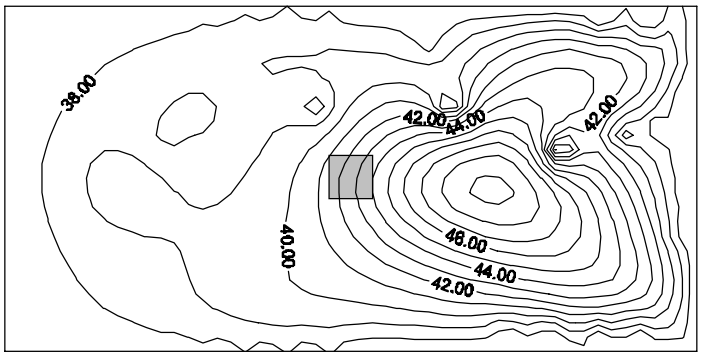

(a)

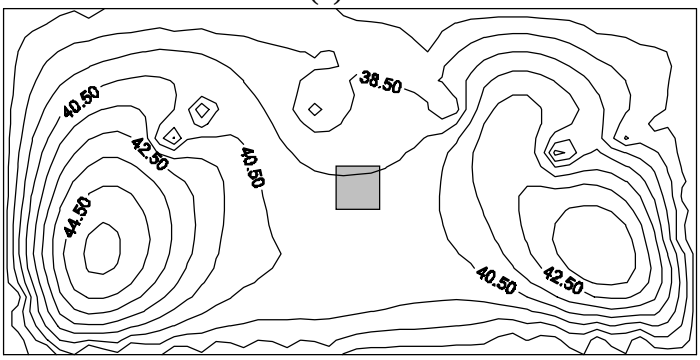

(b)

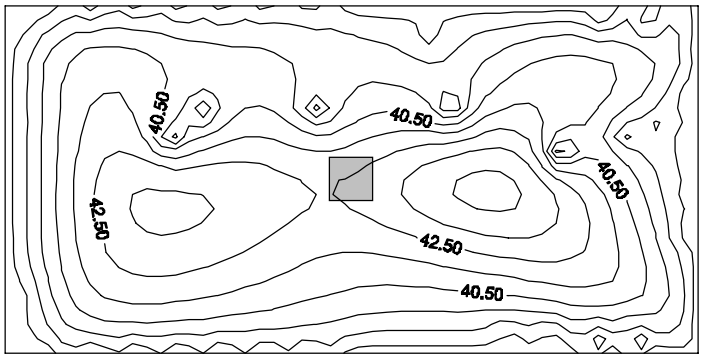

(c)

Figure 4 – Temperature distribution after 2 minutes heating for microwaves inciding at the (a) left , (b) right surfaces and (c) alternating both surfaces each 10 s.

The results presented in Fig. 4 show that temperature distribution is significantly affected by irradiation direction. The temperature distributions presented in Fig. 4 (a) and (b) reveal that higher temperatures were concentrated far from the tumor. Alternating the direction of microwave irradiation (Fig. 4 (c)) resulted in higher temperatures near the tumor, and was more appropriate for the situation represented here. An irregularly shaped tissue sample was also heated under the same conditions of the rectangular sample presented in Fig. 4. The temperature distribution after 2 minutes heating is presented in Fig. 5. In this case, microwave irradiation from the right lead to a satisfactory temperature distribution.These results show that the choice of an effective heating treatment will depend on the sample size and shape, on the size, shape and location of the tumor, and also on the form of irradiation application. Therefore, simulation presents itself as a powerful tool for testing and evaluating several conditions in order to maximize heating at the location of the tumor and minimize heating of heathy tissue.

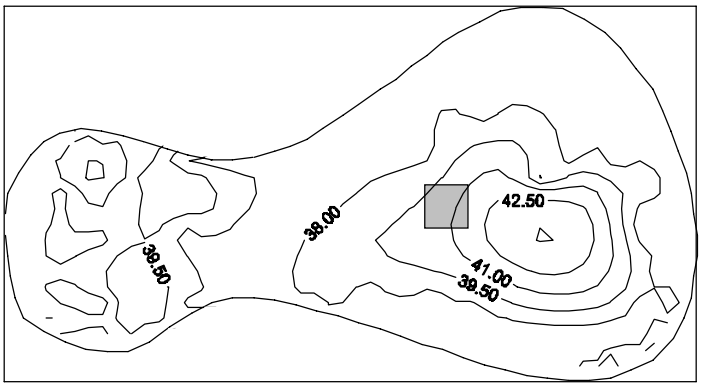

(a)

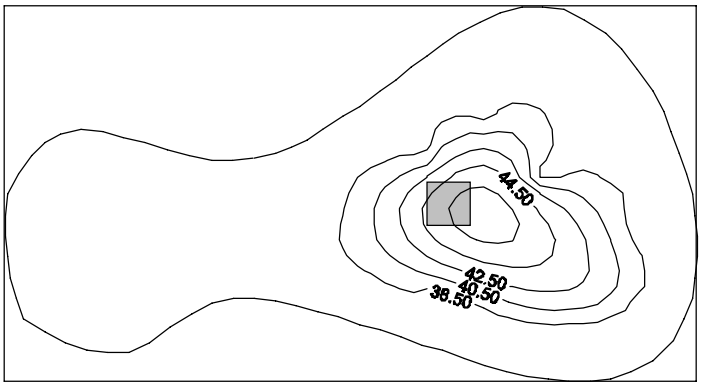

(b)

Figure 5 – Temperature distribution after 2 minutes heating for microwaves inciding at the (a) left and (b) right surfaces.

The effect of microwave power was also evaluated, with results presented in Figure 6. It can be observed that an increase in microwave power results in higher temperatures. These results illustrate the need for rigorous control of microwave intensity, in order to avoid tissue overheating.

The effect of blood perfusion rate was evaluated and the results are presented in Fig.7. The blood perfusion rate can vary depending on tumor location. The results displayed in Fig. 7 indicate that the treatment of tumors located at or near regions with high blood perfusion rates (e.g. arteries) requires higher intensity of microwave power.

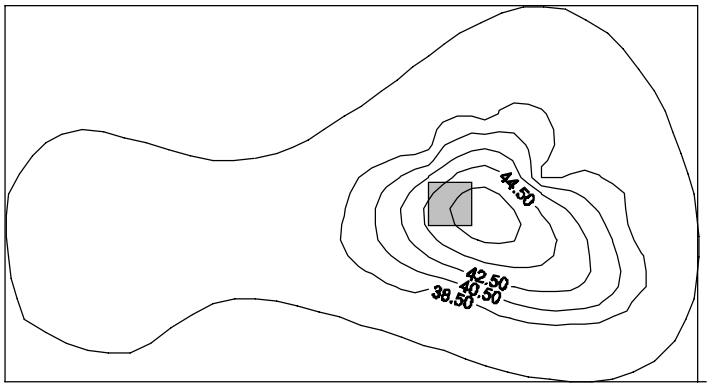

(a)

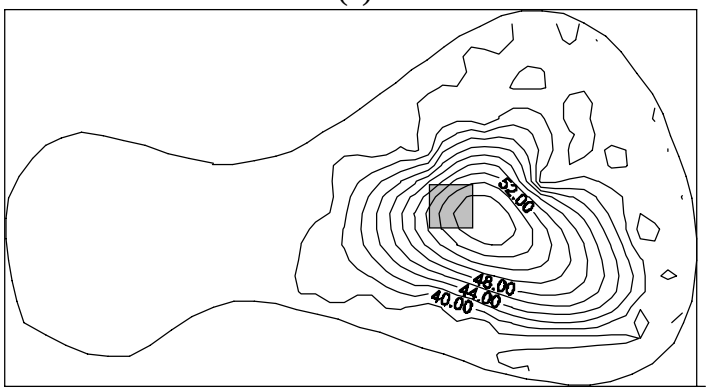

(b)

Figure 6 – Temperature profiles for (a) 0.5 W/cm^2 and (b) 1.0 W/cm^2 microwave intensity.

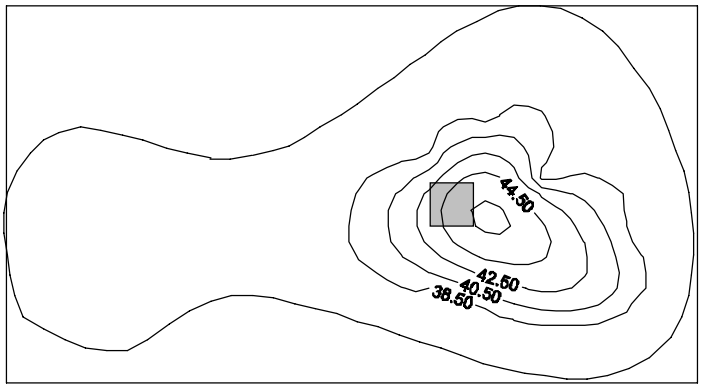

(a)

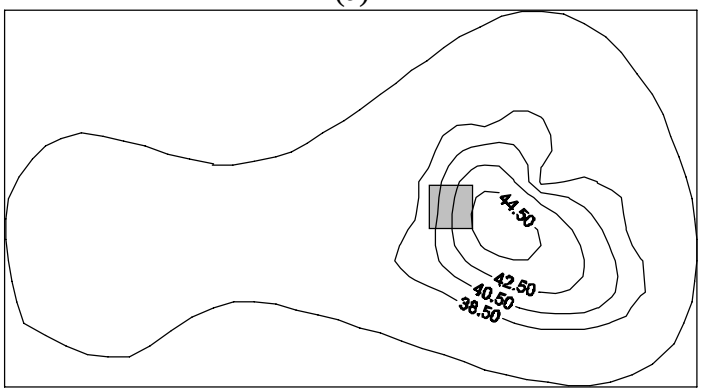

(b)

Figure 7 – Temperature profiles after 2 minutes heating for (a) 0.044 cal/cm^{3}s and (b) 0.25 cal/cm^{3}s blood perfusion rates.

CONCLUSIONS

A simulation study of microwave heating applied to treatment of tumors by hyperthermia was presented. The electric field distribution obtained from solving Maxwell's equations was coupled to the energy equation to predict the temperature distribution during microwave heating. The applicability of Lambert's law approximation was evaluated. Simulation results show that power distributions predited by Maxwell's equations tend to agree with Lambert law predictions as the sample radius increases. However, application of Lambert's equations to simulate hyperthermia is quite restricted. Simulation results have shown that the choice of an effective heating treatment will depend on the sample size and shape, on the size, shape and location of the tumor, and also on the intensity and form of irradiation application. Also, the results indicate that the treatment of tumors located at or near regions with high blood perfusion rates requires higher intensity of microwave power. The results presented in this paper show that simulation is as a powerful tool for testing and evaluating treament conditions.

Acknowledgements

M.E.C. Oliveira acknowledges financial support from CAPES.

REFERENCES

Ayappa, K.G., Davis, H.T., Crapiste, G., Davis, E.A. & Gordon, J., 1991, Microwave heating: an evaluation of power formulations, AIChe Journal, vol. 37, n. 4, pp. 1005-1016.

Ayappa K.G., Davis, H.T., Davis, E.A. & Gordon, J., 1992, Two-dimensional finite element analysis of microwave heating, AIChe Journal, vol. 38, n. 10, pp. 1577-1592.

Balanis, C.A., 1989, Advanced engineering electromagnetics, J. Wiley, New York.

Barringer, S.A., Davis, E.A., Gordon, J., Ayappa, K.G. & Davis, H.T., 1995, Microwave heating temperature profiles for thin slabs compared to Maxwell and Lambert law predictions, Journal of Food Science, vol. 60, n. 5, pp. 1137-1142.

Datta , A., Prosetya, H. & Hu, W., 1992, Mathematical modeling of batch heating of liquids in a microwave cavity, Journal of Microwave Power and Electromagnetic Energy, vol. 27, n. 1, pp. 101-110.

Givoli, D. & and Keller, J.B., 1989, Exact non-reflecting boundary conditions, Journal of Computational Physics, vol. 82, pp. 172-192.

Grote, M.J. & Keller, J., 1995, Exact nonreflecting boundary conditions for the time dependent wave equation, SIAM J. Appl. Math., vol. 55, n. 2, pp. 280-297.

O'Brien, K.T. & Mekkaouni, A.M., 1993, Numerical simulation of the thermal fields occurring in the treatment of malignant tumors by local hyperthermia, Journal of Biomechanical Engineering, vol. 115, pp. 247 –253.

Ramo, S., Whinnery, J.R., & Duzer, T., 1981, Campos e ondas em eletrônica das comunicações, Editora Guanabara Dois, São Paulo.